Computer Vision Techniques for Collision Analysis. A Study Case.

Manta Liviu Florin
Faculty of Automation, Computers and Electronics
University of Craiova
Craiova, Romania
manta@robotics.ucv.ro

Sorin Dumitru
Faculty of Automation, Computers and Electronics
University of Craiova
Craiova, Romania
sorindumitru83@yahoo.com

Dorian Cojocaru
Faculty of Automation, Computers and Electronics
University of Craiova
Craiova, Romania
cojocaru@robotics.ucv.ro

***Abstract*— Following the increased use of mobile platforms, the collision between the mobile platform and elements in its operating environment has become an issue of growing importance. Even if there are extensive researches about the ways to avoid those collisions (sensors, control strategies), in a real-life scenario the dynamics of all the other environmental elements leads to situations when the collision becomes unavoidable. In this paper we proposed, developed and evaluated a test stand for collision analysis, for a previously published theoretical model for planar link in contact with a granular material. The knowledge acquired during this work can be successfully used for impact tests for mobile platforms.**

Keywords*— *computer vision techniques, collision analysis, mobile platforms

I. Introduction

In robotic medical applications, many designers assume that any collision between the links of the robotic arms or parts of the mobile robots, in one side, and the patients or other equipment, on the other side, must be completely avoided. If the joints are equipped with sensors measuring mechanical torque mounted on the motor shaft, then when a collision is detected the movement could be stopped before the motor shaft performs a rotation [1]. Other scientists consider that, when the robotics systems are designed, a potential collision between the robotic arm or parts of mobile platforms (e.g. wheelchairs) and other object outside the patient must be considered. These collisions could affect, and not only indirectly, the patient himself [2, 3]. Even we are focusing only health applications, it may be useful to consider the research already done regarding the impact between many types of surfaces, as they can be parts of the mobile platform, or parts of surrounding environment elements: rod with a flat surface, sphere with a flat, rotor system into a film damper, elastic wedges, solid torus, anisotropic solids, sphere on a beam, anisotropic bi-sinusoidal surface and a rigid base, cylindrical body with a rigid plane [5-8]. It is important also to take into consideration the material properties (incompressible, isotropic, anisotropic, polymers, various finishes). From the point of view of kinematic and dynamic models, it must be considered the influence of the direction of the impact (normal, oblique, normal and tangential) [4]. Usually the study of different types of mechanical impact starts by developing a mathematical model for the specific application. It follows a simulation developed using special scientific programs (e.g. MatLab with Simulink). The next step should be to implement a practical bench and practically verify the results obtained by modeling and simulation. In the study of the mechanical impact, one of the most useful methods are based on computer vision, image acquisition and processing. The successful end of such kind of research should be the validation of the theoretical results by the practical ones. Sometimes the practical results are different from the theoretical expected results. In these cases the cause must be found between the three possibilities: a mistake in the theoretical model, a not enough image acquisition's performance or an inadequate correspondence between the practical bench and the theoretical case under research. This paper presents and discusses a study case of the third type between the upper mentioned ones.

II. Collision Analysis – A Case Study

In order to verify the validity for the theoretical impact models (with emphasis to planar link in contact with a granular material [6]), we designed and realized a test stand, following the steps as in [9]. We drafted a detailed specification for the test stand design, which included (but not limited to): determining the field of view, choosing a proper lens for camera intended to be used, proposing a series of illumination scenarios, choosing software platform and designing relevant data extraction algorithm. On the following paragraphs, we will detail these elements and we will present aspects encountered during data acquisition and processing.

A. Test stand elements and setup

The current collision analysis supposes that we impact the test object against small round plastic particles at certain speeds; for each certain speed, we choose to repeat the impact test for ten times, to observe and compare the post-impact evolutions. In order to attain a good repeatability for impact speed, we needed a launching system which to provide a constant speed; and we concluded that for the current collision analysis, the most efficient in terms of costs and results is to use gravitational acceleration [10, 11], using

$$v\_impact=\sqrt{2gd} \quad (1)$$

where d is the launching height.

Since the test object is made from a ferromagnetic material, we opted for an electromagnetic device as launcher (see fig. 1).

CIDSACTEH, PN-III-P1-1.2-PCCDI-2017-0290, nr. 78PCCDI/2018.

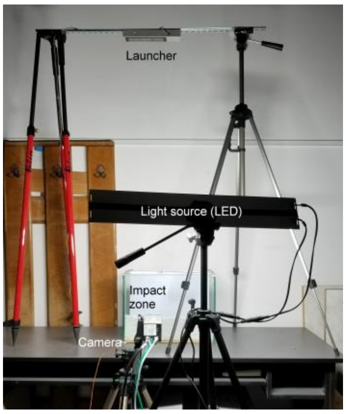

Fig. 1. Experimental test stand: launcher, light source, camera, impact zone.

The height of launcher is adjustable, and we used a laser distance meter to measure the launching height (measured as the distance between the lower tip of the test object, and the plastic particles level). The release for the test object is achieved by activating the launcher.

The plastic particles have a round shape of 6mm diameter, and weights 0.12 grams each. In order to assure a good post-impact visualization, they are placed in a recipient made of safety glass. Before every launch, they are arranged and leveled. One can observe that they are naturally forming a hexagonal network.

As for video camera, we considered two options: a professional Fastec Imaging – InLine High-Speed Camera (further referred as Fastec) and a GoPro Hero 5 Black Edition (further referred as GoPro). The first considered camera, Fastec, can record color videos in following modes: up to 250 fps at a resolution of 640x480 pixels, 500 fps at 640x240 pixels, or 1000 fps at 320x240 pixels [12]. It guarantees a jitter less than 10%, which is essential in the analysis of the test object post-impact movement. The second camera offers better resolutions, as 1920x1080 at 120 fps, 1280x720 at 240 fps or 120fps for different focal lengths [13], but the producer doesn't provide any information about the jitter. In choosing the camera, we considered the following factors:

- Resolution. In our experiment, we need to observe the movement of the test object over 165 mm along vertical axis. For Fastec camera, this gives us a spatial discretization of 0.259 mm per pixel, at up to 500fps (with camera tilted with 90° around its optic axis).

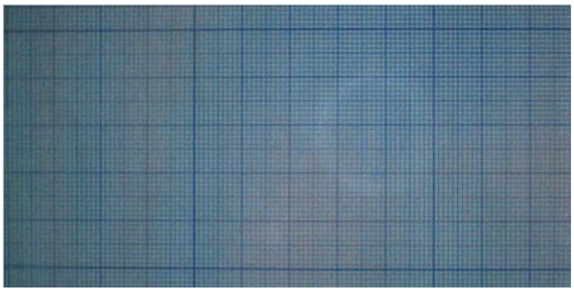

Fig. 2. Image acquired with Fastec camera and Navitar lens. There is no geometric distortion in the image

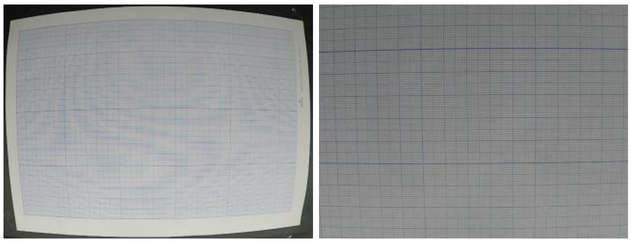

Fig. 3. Image aquired with GoPro at 1920 x 1080 resolution, 14mm focal length (left image, pronounced barrel distortion) and 28 mm focal length (right image, significant barrel distortion).

For GoPro camera, it gives us a spatial discretization of 0.128 mm per pixel, at up to 240 fps, and 0.085mm per pixel, at up to 120 fps. One can observe that a fine spatial discretization can be obtained for the GoPro camera, which made us to consider it as a potential camera. As for pixel aspect ratio, the Fastec camera has an 1:1 pixel aspect ratio in relation with X and Y axis, thus it has a square pixel. No information is given about the GoPro pixel aspect ratio.

- Time sampling. Given the estimated impact process speed, we considered 3 time sampling values: ~125 fps, ~250 fps and 500fps [14]. Both Fastec and GoPro cameras can be used for 125 and 250 fps, but only Fastec can acquire images at 500 fps. As previously stated, the jitter is known for Fastec camera, and not specified by producer for GoPro Camera.

- Lens. For Fastec camera, we can use any lens with C-mount. For the current experiment, taking into account the experiment characteristics, we opted for a Navitar 12mm focal lens. Since we will acquire images at up to 500fps, and the relevant depth of field can be narrow, we opted for a 1.2 F number in order to have brighter images. The chosen lens presents no significant geometrical distortion, as can be seen in fig. 2. For GoPro, we can use only factory-mounted lens, but with options on selecting the field of view (FOV)/focal length: 14/28mm software selectable for 1920x1080 at 120 fps, 28mm for 1280x720 at 240 fps, 14/21/28 mm software selectable for 1280x720 at 120 fps. Also its lens are prone to geometric distortion, as can be seen in fig. 3 and fig. 4.

- Recording format and available memory. The Fastec camera embeds 512MB of memory, used to record up to 8 seconds at 500fps, with a resolution of 640x240, in a raw (uncompressed) format.

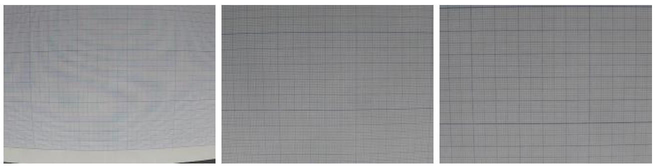

Fig. 4. Image aquired with GoPro at 1280 x 720 resolution, 14mm focal length (left image, pronounced barrel distortion), 21 mm focal length (central image, significant barrel distortion) and 28 mm focal length (right image, slight barrel distortion).

The GoPro can record only compressed videos (h.264 codec on MP4 file format, maximum bitrate 60Mbit/second), and the time of recording depends on the size of memory card (multiple of tens of minutes). Given the fact that the collision event has a short duration, the record time is not a parameter to consider, but the fact that Fastec can record uncompressed videos while GoPro can record only compressed videos is to be taken into account, since, obviously, compression induces an important decrease of video quality.

- Dimensions, weight, autonomy, vibrations. Being a scientific purpose camera, the Fastec camera requires a tripod to be mounted on, external power supply, Ethernet connection to a computer in order to be controlled, it weighs 500 grams and is 170mm long (without lens). The GoPro camera is smaller, lighter (117 grams), has an internal power supply (battery), can be wirelessly remote controlled, it can sustain prolonged vibrations (being an action camera purpose) and the producer offers a large variety of mounting solutions.

As a conclusion, although the GoPro's spatial discretization is very attractive (main reason for considering it as an option), all the other aspects disqualifies it as a camera which can be used in the current scientific experiment. But, for future impact tests which may imply the mounting on mobile structures (robotic arms or mobile robots), it might be worth it to make some evaluations and calibrations of the GoPro camera, in terms of jitter and image geometric properties, to explore if it may be used as a reasonable priced scientific tool.

There are also other aspects to be taken into consideration, other than the ones related to lens and image processing. An important influence on the result of the experiments is given by the illumination aspects. Insufficient illumination will limit the acquisition rate, and also will affect the quality of acquired images; excess of light and unstable lighting will develop into later image processing complications.

Ideal is to place the source of light as possible close to the area captured in the image, since the brightness will decrease with the square of the distance (measured between the light source and the area captured in the image) – but the drawbacks must me very well taken into account – unwanted and powerful reflections, which will generate overexposed regions in acquired image, and also uneven illumination dispersion – powerful light in center image, considerably less to the image margins.

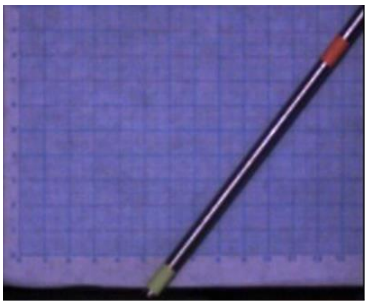

Fig. 5. Green and orange markers placed on the test object, to identify the relevant points – calibration phase.

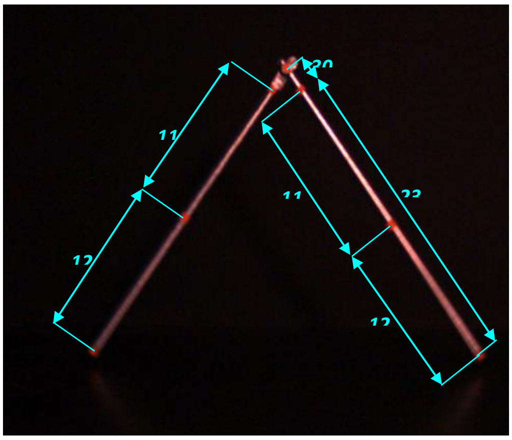

Fig. 6. Using markers to identify relevant points in image – the experiment phase; example for a two articulated bars used to impact a surface.

Considering the spectrum (ultraviolet - UV, visible - VIS, infrared - IR), or the color temperature (for VIS light), the next choice is the type (bulb, tube, LED) and power of light. The classic electric bulb will provide average results from all point of views: color temperature (rich on the red and IR end of VIS spectrum), weak performance as intensity / heat / consumed power aspects, flickering effect if not powered by a stable DC power source. The tungsten/halogen bulb presents better performances than the classic bulb in terms of light intensity and color temperature, but the generated heat is considerable higher. For a long period of time, it was a good choice (along with a good DC source) for industrial and research experiments, in which a small field of view was used. Xeon bulbs provide higher light intensity, better color temperature, medium dissipated heat.

A well-known phenomena is the 20KHz flickering, but can be tackled in terms of acquisition rate and exposure time, in such way to no produce flickering in acquired images. Another option is represented by HMI (Hydrargyrum medium-arc iodide) light sources - they are expensive and have a high operating temperatures, but offers good light intensity, reach and stable color temperature, and they don't present flicker. In the latest years, the LED technology advanced enough to offer good color temperatures, relatively cold operation, and stable light (when a good DC current power source is used). Also, current LED light sources actually uses a large number of LED's, distributed over a given area. This enables a uniform light dispersion, without powerful shadows and reflections.

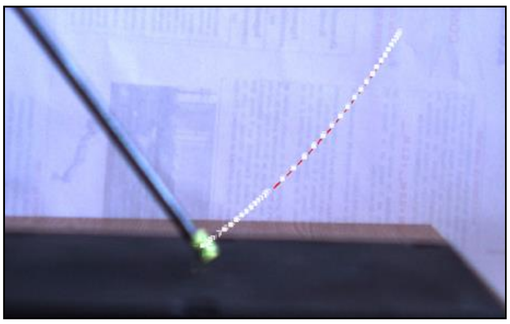

Fig. 7. Using markers to track the relevant points movement in image; example for one bar impacting a surface.

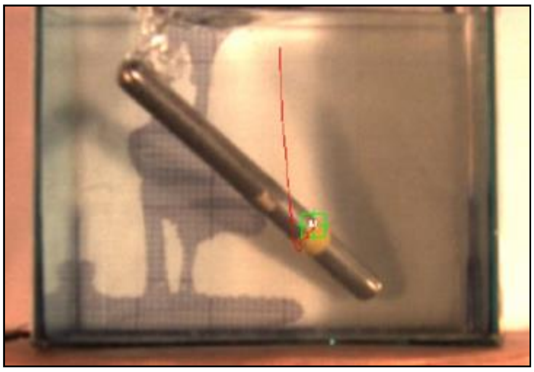

Fig. 8. Using markers to track the relevant points movement in image; example for one bar impacting a fluid in a reservoir.

One way to identify the relevant positions on impacting bodies is to place color markers, reflexive or non-reflexive ones, on their surface, as shown on fig. 5 and fig. 6. In this type of application, from the point of view of image processing, a performed procedure is needed in order to identify the center of the markers. Taking into consideration the illumination conditions and the high speed of the image acquisition this task is not an easier one if we impose a low rate, less than one pixel.

In our application, the test object motion is observed by using markers to track its movement. Fig. 7 and fig. 8 shows the movement tracks, as determined from recorded images, based on applied markers. In order to achieve the best separation of the markers against the background, we considered to evaluate all the three general ranges of the electromagnetic spectrum [15]: UV light, visible (VIS) light and IR light, in order to obtain the best separation of markers against the background. We applied appropriate markers (with good reflectivity on UV / VIS / IR light, at a time) on the test object, and applied the corresponding light. The test runs revealed that the Fastec camera has filters applied on imaging sensor, which completely cuts the UV and IR spectrums (information not provided by the camera producer), thus we can use only the VIS spectrum. In VIS spectrum, we opted to use HSL color representation, since it separates the hue and the lightness [16]. After testing several colors for markers, we noted that the best separation against the background on HSV color space is for H=112 – green, thus we applied green two markers on our test object, as a band around the bar, placed at 90mm and 140mm from the lower tip of the test object. We used two markers, in order to also determine the post-impact inclination of the test object.

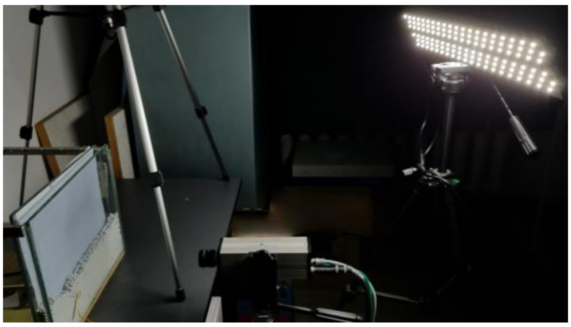

Fig. 9. Light source used for scene illumination.

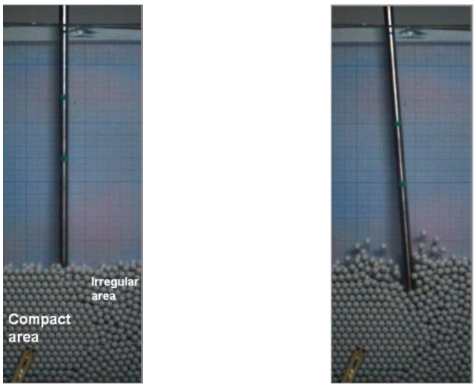

Fig.10. a) On the left side of the image, the particles are arranged and forms a compact region; on the right side, their placement is irregular. The test object impacts the plastic particles right on the separation zone between the two region.

Fig.10. b) The test object path is reoriented by the border between the two regions. A gap between the two regions it formed, and it favors a deeper penetration of the test object.

As VIS lighting system, we opted for two LED rectangular panels (60 SMD LEDs on each panel), providing white light and powered by constant current source. We have chosen this type of light because is stable in time (no oscillations / fluctuations on neither lightness nor hue), is compact and powerful, and the shape of the panel (in correlation with its mounting) eliminates the shadows and unwanted reflections in image, thus assuring optimal illumination of the observed scene, as seen in fig. 9.

Related to software platform, since a real-time processing of the information is not needed, we opted for MATLAB environment, as a powerful platform for image processing. The relevant data is extracted as markers centroid positions in X and Y pixel coordinates [17].

Using a calibrated image, we converted that information in metric distances. The image processing is made following several steps:

- First, we open the video file and determine its resolution (in pixels) and length (in number of frames)
- For each frame, we convert the image from RGB color space to HSV representation
- We determine a threshold value in HSV color space and impose it in such way that all the relevant (marker) pixels, in terms of hue of markers, to be selected from the area of interest. Then we change the intensity of each selected pixel to a fixed, known value
- We filter the image for small regions of selected pixels, since they represent noise in image, and not pixels of the proper marker
- Inside the identified markers, we fill the small regions represented by not-selected pixels
- We extract the centroid positions for the two marker regions, in (X,Y) positions, and the inclination of the test object
- We save the extracted information for all the frames, in order to analyze the post-impact evolution.

B. Aspects encountered during tests

When using a high speed camera for measuring the velocity in experiments for the study of the mechanical impact, there are several sources of errors [18, 19]. The first cause of error, as previously stated, is the jitter – the variation of time between two consecutive frames. Since the jitter it has a constant value, when the frame rate increases, the error induced by jitter also increases.

Is the main reason why we chosen the Fastec camera – it has a known jitter. Another source of errors is the uncertainty in determining the markers (centroids) positions. This error can be approached by reducing the exposure time per frame; this can be done by assuring a bright and good illumination system – that's the main reason why we opted for the LED lighting solution. Another source of error is due to speed / acceleration of object between two frames – the higher the framerate, the lower effect of acceleration can be observed. This aspect will be detailed in the following paragraphs.

Once the test stand was ready, we proceeded to impact the test object against the plastic particles at different speeds, ten launches for every speed.

One of the first observations made during tests, is that the arrangement of plastic particles, a priori to impact, have a great influence on post-impact evolution. If the particles are arranged in an irregular manner, it influences the post-impact direction, depth and speed evolution of the test object, as in fig. 10. Analyzing the data shown in fig. 11 and 12, one can observe that the gap described in fig. 10. b) allow the test object to slide almost frictionless amid plastic particles, and at 64 milliseconds (8 frames) since impact the gravitational acceleration even generates a temporary increase of speed. The data shown in fig. 7 was acquired at 250 FPS, for a drop height of 360mm. Thus, before every test, we rearranged the plastic particles in a regular pattern. Also one can note that the speed / acceleration profile after the impact weren't smooth enough, so we decided to acquire data at 500 fps.

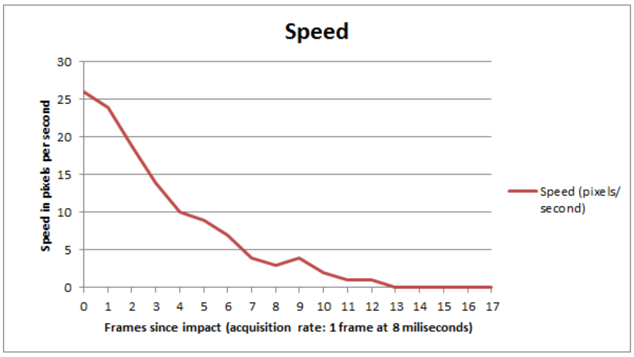

Fig. 11. Speed evolution of test object, measured as displacement difference expressed in number of pixels, for 250 fps and 360 mm drop.

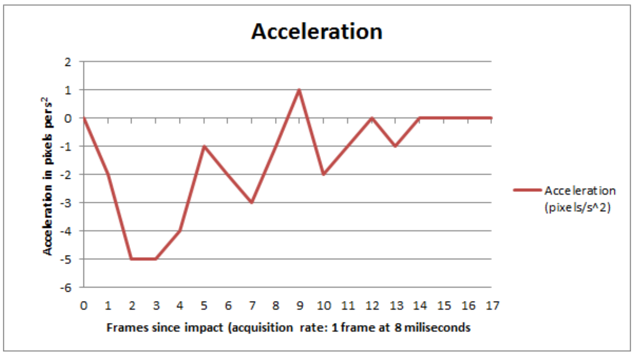

Fig. 12. Acceleration evolution of test object, measured as displacement difference expressed in number of pixels, for 250 fps and 360 mm drop.

Another observation was made after processing higher volumes of recorded data. In the moments after impact, the movement of the test object is fast and requires a high number of frames per second in order to have a good representation of its movement. But at the end of post-impact evolution, the movement of the test object is too slow and under pixel resolution. In fig. 13 is represented the data recorded for a drop of 580 mm height, captured at 500fps.

As previously stated, the spatial discretization is 0,259 mm/pixel, which means that a one pixel displacement on the image equals a speed of 129.5 mm/s.

One can observe that after frame no. 19 since impact, the speed between two consecutive frames is 3 pixels, and then lowers to 2 pixels (after frame no. 30) and so on.

As previously stated, this means that in this part of post-impact evolution, the spatial discretization (camera resolution) is too low to capture the change in speed of the test object – the higher framerate/lower speed phenomena occurs. One can only estimate the instantaneous speed using non-linear interpolation

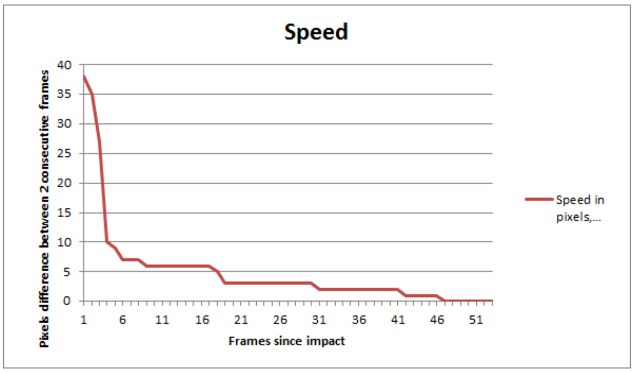

Fig. 13. Speed evolution of test object, measured as displacement difference expressed in number of pixels.

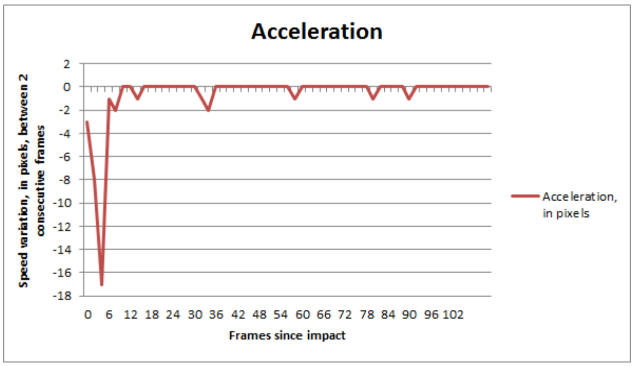

Fig. 14. Acceleration evolution, measured as speed variation in pixels

based on trending of sample data. Also, when computing acceleration, this phenomena leads to high discontinuities in acceleration evolution – see fig. 14. As solution, we considered as valid data only the displacement, and for speed we imposed a threshold (3 pixels between 2 consecutive frames) when to consider the data as being relevant.

Having established the test stand and approached the sources of possible induced errors, we conducted more than 60 launches and impact analyses to test theoretical impact models.

III. Conclusions

In this paper we presented a case study of how to design a collision analysis video stand to be used for the validation for theoretical impact models. We presented the test stand in terms of hardware and software elements, and we offered reasoning for the way we choose them. Then we used the test stand to verify the impact model for planar link in contact with a granular material [6]. In this sense, we conducted more than 60 launches from different launch height, and we analyzed the data,. For future work, we will change the impact setup, and test for other type of particles (different sizes, weights and materials for the particles). Also, the expertise gained during those experiments can be used in analyzing other type of mechanical impact studies, like impact of mobile platforms with different elements in its operating environment.

Acknowledgment

The results presented on this paper were partially supported from the funds of complex research project "Intelligent and distributed control of 3 complex autonomous systems integrated into emerging technologies for personal medical assistance and precise flexible manufacturing service (CIDSACTEH)", financed by PN III scheme, program 1 – Growth of national research and development system, sub-program 1.2 – Institutional performance. The research project code is PN-III-P1-1.2-PCCDI-2017-0290, and the financing contract for execution in RDI Complex Projects is registered with no. 78PCCDI/2018 at UEFISCDI.

References

[1] F. Pierrot, O. Company and S. Krut, A Few Guidelines A Few Guidelines for the for the Design of Surgical Robot Arms, Summer School on Surgical Robotics, LIRMM, CNRS & University Montpellier 2, 2007

[2] G. H. Ballantyne, "Robotic surgery, telerobotic surgery, telepresence, and telementoring," Surg. Endoscopy, vol. 16, pp. 1389–1402, 2002

[3] S. Haddadin, A. De Luca, A. Albu-Schäffer, "Robot collisions: A survey on detection, isolation, and identification," IEEE Trans. on Robotics, vol. 33, no. 6, pp. 1292-1312, 2017.

[4] G. Hamid, O. Cermik, D. B. Marghitu, K. Kardel, "Collision Measurements Using Digital Image Correlation Techniques", International Journal of Mechanical Sciences, 131-132: 836-846, 2017

[5] D.B. Marghitu, D. Cojocaru, R.L. Jackson, "Elasto-Plastic Impact of a Rotating Link with a Massive Surface", International Journal of Mechanical Sciences, ISSN: 0020-7403, Volume 53, Issue 4, Elsevier, p309-315, April 2011

[6] D.B. Marghitu, L. Seunghun, D. Cojocaru, "Stopping Time for a Planar Link in Contact with a Granular Material", Annals of the University of Craiova – Series: Automation, Computers, Electronics and Mechatronics, Editor: University of Craiova, Editura UNIVERSITARIA Craiova, Romania, vol. 11(35) , No. 1 - 2011, p21-26, ISSN: 1841-0626, 2011.

[7] D.B. Marghitu, D., Cojocaru, "Simultaneous Impact of a Two-Link Chain, Nonlinear Dynamics", An Intrnl. Journal of Nonlinear Dynamics and Chaos in Eng. Systems, Springer Ed., ISSN:0924-090X, Volume 77, Issue 1-2, pp 17-29, 2014

[8] D. Cojocaru, D.B., Marghitu, "Differential Formulation for the Coefficient of Restitution of a Rigid Link", Applied Mechanics and Materials, ISSN: 1660-9336, Vol. 762, Mechatronics and Robotics, ISBN-13: 978-3-03835-444-4, Trans Tech Publications, p175-183, Switzerland, 2014.

[9] A. Hornberg, Handbook of Machine Vision, Print ISBN:9783527405848, Online ISBN:9783527610136, DOI:10.1002/9783527610136, 2006 Wiley-VCH Verlag GmbH & Co. KGaA.

[10] N. Banthia, S. Mindess, A. Bentur, M. Pigeon, "Impact testing of concrete using a drop-weight impact machine", Experimental Mechanics vol. 29, pag. 63, https://doi.org/10.1007/BF02327783, Kluwer Academic Publishers 1989.

[11] J.D.Winkel, D.F.Adams, "Instrumented drop weight impact testing of cross-ply and fabric composites", Composites Volume 16, Issue 4, pag. 268-278, https://doi.org/10.1016/0010-4361(85)90279-4, Elsevier Ltd. 1985.

[12] Fastec Imaging – InLine High-Speed Camera user manual

[13] GoPro Hero 5 Black Edition user manual, https://gopro.com/content/dam/help/hero5-black/manuals/HERO5Black_UM_ENG_REVC_Web.pdf

[14] V. L. B. de Jesus, Experiments and Video Analysis in Classical Mechanics, DOI: 10.1007/978-3-319-52407-8, Springer International Publishing, 2017

[15] I. Jahr, "Chapter 3 - Lighting in Machine Vision", Handbook of Machine Vision, 2006 Wiley-VCH Verlag GmbH & Co. KGaA

[16] G. Siogkas, "Visual Media Processing Using MATLAB", ISBN 978-1-84969-720-0, Packt Publishing, 2013

[17] Y. Chen, Y. Xie, Y. Wang, Yulin, "Detection and recognition of traffic signs based on hsv vision model and shape features". Journal of Computers, 2013, DOI: 8.10.4304/jcp.8.5.1366-1370.

[18] Y. Fenga, J. Goree, B. Liu, "Accurate particle position measurement from images", Review of Scientific Instruments 78, 053704 (2007); https://doi.org/10.1063/1.2735920, 2014.

[19] Y. Feng, J. Goree, B. Liu, "Errors in particle tracking velocimetry with high-speed cameras", The Review of scientific instruments 82(5):053707, DOI 10.1063/1.3589267, 2011.